AJNR

Semilobar Holoprosencephaly Seen with Diffusion Tensor Imaging and Fiber Tracking

Nancy Rollins

AJNR Am J Neuroradiol 2005, 26 (8) 2148-2152
http://www.ajnr.org/content/26/8/2148

This information is current as of August 12, 2025.

AJNR Am J Neuroradiol 26:2148–2152, September 2005

Case Report

Semilobar Holoprosencephaly Seen with Diffusion Tensor Imaging and Fiber Tracking

Nancy Rollins

Summary: A neonate with semilobar holoprosencephaly was studied with diffusion tensor imaging and fiber tracking. Fiber tracking showed that the frontooccipital fasciculi were in continuity across the ventral midline, interposed between fused caudate and dysplastic fornices. Tractography of the posterior limbs of the internal capsules showed fibers arching ventrally toward the expected location of the motor cortex; some fibers also coursed dorsally, presumably to the sensory cortex. There was a posterior commissural white matter bundle representing a callosal splenium. Diffusion tensor imaging and fiber tracking revealed white matter structures not apparent on routine imaging sequences, which are in agreement with pathologic descriptions of the holoprosencephalic brain.

Diffusion tensor imaging is a relatively new MR imaging technique in which image contrast is provided by diffusion anisotropy, the inherent preferential directional movement of water within the brain (1–6). Diffusion tensor imaging provides information about white matter organization and architecture not possible with conventional MR imaging (5, 6). Diffusion tensor data are displayed as 2-dimensional color maps in which image brightness indicates diffusion anisotropy and color indicates tract orientation (1–6). Fiber tracking may be performed by defining a region of interest on the color maps or fractional anisotropy maps and interrogating the regions of interest for fibers having a minimal fractional anisotropy set by the user (4–6); the resultant 3D image shows axonal projections. Diffusion tensor imaging and fiber tracking can be used to study congenital brain malformations. Holoprosencephaly is a complex forebrain anomaly; approximately 25% of holoprosencephalic brains are of the semilobar form (7). Diffusion tensor imaging has been used to study brain stem white matter tracts in patients with various forms of holoprosencephaly (8), although fiber tracking has not, and, to our knowledge, there are no reports on the use of fiber tracking in the supratentorial white matter of the holoprosencephalic brain. We report diffusion tensor imaging and fiber tracking in a neonate with semilobar holoprosencephaly.

Received September 18, 2004; accepted after revision December 3.

From the Department of Radiology, Children's Medical Center and the University of Texas Southwestern Medical Center, Dallas, TX.

Address correspondence to Nancy Rollins, Department of Radiology, Children's Medical Center, 1935 Motor Street, Dallas, TX 75235.

© American Society of Neuroradiology

Case Report

A 2.9-kg 6-day-old white male neonate presented with dehydration and irritability and was found to have diabetes insipidus, hypoglycemia, and hypothermia. The infant was the product of a nonconsanguineous marriage between healthy parents and had been delivered at 39 weeks by elective cesarean delivery after an uncomplicated full-term pregnancy. There was no family history of birth defects or neurologic problems. There were 3 normal male siblings. The patient had normal limbs and genitalia and no evidence of congenital heart disease. There was microcephaly, a shallow sloping forehead with hypotelorism, midface hypoplasia, and a high-arched but intact palate. Routine chromosomal analysis showed a normal male karyotype. No further genetic analysis was performed.

Diffusion tensor imaging was performed in accordance with the institutional investigational review board. MR imaging was performed with the patient under conscious sedation, using a 1.5-T MR unit (Intera Release 9, Philips Medical Systems, Best, the Netherlands) with 30 mT/m gradients and slew rate of 150 T/m/msec, using the standard quadrature headcoil operating in receive mode. Conventional MR images included sagittal and coronal T1-weighted spin-echo sequences (TR/TE/signal intensity averages, 400/25/2) and axial T2-weighted fast spin-echo (TR/TE/signal intensity averages, 4500/90/3). Diffusion tensor imaging was performed with a 6-channel sensitivity encoding headcoil operating in receive mode, applying high angular resolution diffusion imaging (2) isotropic diffusion-weighted gradients, using a single-shot spin-echo planar sequence with a sensitivity encoding factor of 2.5 and an echo-planar imaging factor of 35. Other parameters were the following; b = 700; TR/TE/ signal averages, 7357/98; scan matrix, 112 × 256; 246 × 246 mm field of view; 55 sections; 2.2-mm section thickness; no gap; and 15 diffusion-weighting directions. The diffusion tensor imaging sequence was repeated 3 times using 1 signal-intensity average for a total image acquisition time of 7 minutes.

The raw data from the diffusion tensor imaging sequences were transferred to an off-line PC having Philips Research Integrated Development Environment (PRIDE) software version 4.1.V3 for image registration and fiber tracking. The 3 diffusion tensor imaging raw datasets were processed by using the Diffusion Registration Tool Release 4 (Philips Medical Systems, Best, the Netherlands). We performed automated section-by-section registration for each individual acquisition, correcting for motion between sections and between acquisitions. The 3 corrected datasets were averaged together and saved as a new raw data file. Fiber tracking was generated using the fractional anisotropy continuous tracking algorithm (4). Tracking was initiated by manually placing a region of interest within regions of the brain showing high fractional anisotropy or color on the fractional anisotropy and color maps, respectively. Tracking was performed from all pixels inside the regions of interest using a "brute force" approach. Tract propa-

gation was terminated at a fractional anisotropy value of 0.15 and when the internal angle was 0.75°.

Results

The sagittal T1-weighted images showed relatively normal infratentorial structures. There were no discrete callosal fibers identifiable. The fused caudates were seen ventral to the fused thalami (Fig 1*A*). On the axial T2-weighted images (Fig 1*B*), the ventral neocortex and white matter were fused; there was no anterior interhemispheric fissure. The posterior interhemispheric fissure was present. The sylvian fissures were medial and rostral in position; the claustrum was not visible. The caudates were fused into a crescent-shaped mass straddling the midline (Fig 1*B*). There were no lentiform nuclei. The thalami showed minimal cleavage; the anterior third ventricle was absent, whereas the most posterior recess of the third ventricle and the cerebral aqueduct were patent. There was no hydrocephalus or dorsal cyst. The sulcal pattern was diffusely abnormal with widened gyri throughout most of the brain. The fused thalami were featureless, and the hippocampi were incompletely folded.

The color maps showed a thick bilobed subfrontal structure; the red color indicated a preferential transverse orientation. This bilobed structure was composed of the fused caudates and a transversely oriented white matter bundle. The corticospinal tracts abutted the dorsal surface of the transversely oriented white matter bundle, and a crescent-shaped bundle of transversely oriented white matter fibers was seen in the expected location of the callosal splenium. Bands of green were seen along the ventricular margins, indicating fibers oriented anteroposteriorly and consistent with the frontooccipital fasciculus. Tractography showed the transversely oriented fibers dorsal to the caudate mass connected to the frontooccipital fasciculus across the ventral midline. There was no demarcation between fibers of the inferior and superior frontooccipital fasciculi (Fig 1*C*). There was a discrete callosal splenium. The corticospinal tracts were seen arching ventrally; additional fibers from the posterior limb of the internal capsule coursed dorsally. The fused caudate mass was seen with fiber tracking as a triangular structure, not in continuity with regional white matter (Fig 1*D*).

The coronal image from the fractional anisotropy map showed curved structures of higher fractional anisotropy embedded within and curving through the superior substance of the thalami. Tractography showed thickened dysplastic fornices that were foreshortened in an anteroposterior direction (Fig 1*E*) but that maintained the C-shaped configuration characteristic of fornices as seen by fiber tracking in the normal brain (4, 6). The rostral extension of the fornices divided into horizontally oriented asymmetric paramedian structures, similar to the posterior projections of the anterior commissure, and a single median structure, similar to the precommissural fornix, but thicker and longer than the usual appearance of the precommissural fornix in a neonate. A band of transversely oriented white matter was also seen by tractography over the frontal convexity (Fig 1*F*).

Discussion

Reported here is a neonate with semilobar holoprosencephaly in whom the holosphere was studied using diffusion tensor imaging and fiber tracking. Diffusion tensor imaging and fiber tracking provide a unique means of studying white matter structures and connectivity in the intact brain, unmarred by fixation and dissection artifacts, and these techniques have enormous potential application in complex congenital brain malformations. Diffusion tensor imaging characterizes the 3D movement of water (1–6). Directionality is specified by the eigenvectors, whereas the eigenvalues specify the rate of diffusion (1). The 2-dimensional color maps show the eigenvectors associated with the highest eigenvalues; color is used as an indicator of fiber orientation (2, 3). On the anisotropy maps, regions of brain having high degrees of spatial anisotropy are seen as regions of increased signal intensity. In the normal neonate, spatial anisotropy within white matter is relatively low (9, 10). Although it was initially proposed that myelin was obligatory for anisotropic water diffusion across the axon, it is now known that diffusion anisotropy can be seen in unmyelinated white matter tracts (9, 10).

Other determinants of diffusion anisotropy include tissue hydration, cell-packing attenuation, fiber diameter, attenuated axon packing, and axonal substructures such as membranes, microtubules, neurofilaments, microfilaments, as well as nonstructural metabolic activities such as axonal transport and cytosolic streaming (3, 9, 10), all factors that allow diffusion tensor imaging and fiber tracking to be used to study the immature brain. Gray matter also possesses some degree of inherent anisotropy that is normally lower than that in white matter because of the extensive intrinsic axonal and dendritic branching (10, 11). Nonetheless, densely packed neurons embedded in highly organized glial fibers may show high fractional anisotropy such as in the fetal cerebral cortex or in the cortex of the lissencephalic brain (12, 13). Although histologic correlation is not available, the relatively high fractional anisotropy of the fused caudates seen in the patient reported here may be explained on the basis of densely packed highly organized neurons and axons.

Holoprosencephaly is the most common anomaly affecting the ventral forebrain, occurring in 1/250 embryos and 1/8300–16,000 live births (14, 15). Holoprosencephaly is notable for its genetic heterogeneity; at least 12 holoprosencephaly loci have been identified that play some role in the pathogenesis of holoprosencephaly, including Shh, Otx2, Emx, Pax, Nkx-2.2, and some POU domain genes that participate in inductive signal-intensity transduction (15–17). Although 24%–45% of affected live-born individuals have chromosomal abnormalities, there is no known correlation between the type or severity of the holoprosencephalic defect and the location of the

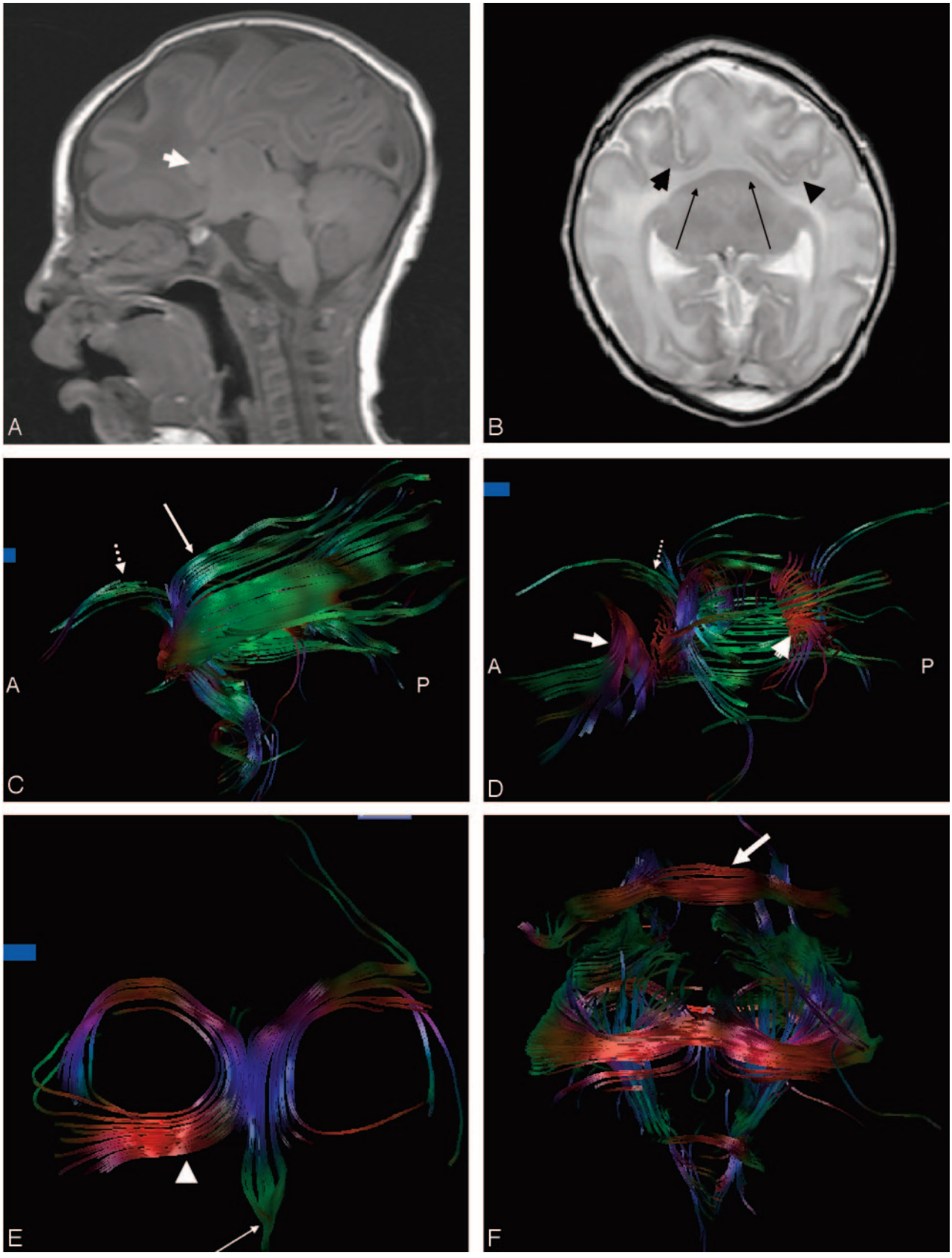

FIG 1. *A*, Sagittal T1-weighted images show preservation of the infratentorial contents. There is no third ventricle or definite callosal fibers. Arrow indicates fused caudates.

B, Axial T2-weighted image shows marked frontal lobe hypoplasia resulting in anterior and medial displacement of the sylvian fissures (*arrowheads*). The fused crescent-shaped caudates are indicated by the arrows. Note the fused thalami.

holoprosencephaly gene (14–17). Sonic hedgehog (Shh), the first holoprosencephaly gene identified, is expressed in the midline of the developing nervous system. Holoprosencephaly is thought to be due to deficient or defective prechordal mesoderm in which Shh is expressed, with resultant failure of induction or abnormal fusion of normally paired and separate neocortex, caudates, and claustrum (15–18). The consequences of inductive failure of the median and paramedian structures are most pronounced in the ventral forebrain and decline in severity from rostral to caudal and from median to lateral (16). Hence, the lateral cerebral convexities and parietooccipital regions tend to be less severely affected than the frontal lobes (14–18). In addition to controlling prosencephalic separation and differentiation, the inductive effects of the prechordal mesoderm also influence the volume of the ventral forebrain, presumably accounting for the marked frontal lobe hypoplasia seen in holoprosencephaly (16).

There is considerable topographic variation in holoprosencephaly, which is most often characterized as alobar, semilobar, or lobar (7, 18–22). The hallmarks of semilobar holoprosencephaly, seen by routine MR imaging, include relative preservation of the lateral and posterior cerebrum; in the absence of a dorsal cyst, the presence of a splenium-like structure; and preserved posterior interhemispheric fissure and falx associated with a hypoplastic undivided frontal lobe (18–22). Lack of formation of the frontal lobes results in the anterior position of the sylvian fissures, termed a "wide sylvian angle" by Barkovich et al (18). The globus pallidi are absent or hypoplastic, and the caudate nuclei are fused, resulting in obliteration of or lack of formation of the septal region (21). The posterior limbs of the internal capsules are ventral to partially or totally fused thalami (18, 20, 22). The hippocampus is virtually always present, although usually incompletely or abnormally developed (20, 22). Using the criteria described by Takahasi et al (16), who studied 7 patients with semilobar holoprosencephaly using MR imaging–based topologic and morphogenetic analysis, we found that the patient reported here had grade 2 semilobar holoprosencephaly with partial interhemispheric fissure. There was no hydrocephalus and, therefore, no clastic effects on the white matter tracts of the holosphere that might have confounded the diffusion tensor images and fiber tracking.

The use of fiber tracking resulted in visualization of large white matter tracts that were not apparent on routine MR imaging. There were large symmetric fiber bundles having the expected course of the frontooccipital fasciculus; the fasciculus was connected across the midline in the subfrontal region. A smaller transversely oriented fiber bundle was also seen within the higher convexity white matter; this fiber bundle showed no visible continuity with the frontooccipital fasciculus. There was no discrete rostrocaudally aligned midline gray matter seam described by Takahashi et al (16) in their analysis of 7 cases of holoprosencephaly of the semilobar type.

The fornix in the normal brain is composed of 2 crura, joined by a thin hippocampal commissure, the body, and 2 columns (11, 23). Each column normally divides into the pre- and postcommissural fornices; the location is defined relative to the anterior commissure (11, 23). The postcommissural fornix normally extends from the fornical columns to the mamillary bodies, and along with the mamillothalamic tracts are major white matter tracts in the hypothalamus. The precommissural fornix is normally smaller than the postcommissural fornix and extends into the septal, lateral preoptic, diagonal, and anterior thalamic nuclei (11, 23). The precommissural fornix is readily depicted with tractography, whereas the postcommissural fornix is not. Takahashi et al (16) and Probst (20) have stated that the fornices are absent in holoprosencephaly, whereas other investigators have commented that the fornix is present, although frequently hypoplastic or malformed (7, 19). Yakovlev (22) noted a specimen of semilobar holoprosencephaly in which "the alveus and the fimbria of the hippocampal formations formed a massive fornical system of hippocampal projection fibers . . . arching over the thalamus. The fibers of the fornix remained in the wall of the holosphere and were traced dorsolaterally converging forward and then centrally upon the septohypothalamic region behind the corpora striata." This pathologic description of the fornices also identifies the fornices seen by fiber tracking in the patient reported herein. The precommissural fornix was abnormal in appearance; the marked thickening may be related to failure of the fornical columns to divide into pre- and postcommissural portions or to the presence of the "median septohypothalamic mass" described by Yakovlev (22). The location of the precommissural fornix dorsal to the fused caudates seen by tractography is also supported by Yakovlev's examination of pathologic specimens (22). The ante-

C, On the sagittal image derived from fiber tracking, there is no demarcation between the inferior and superior longitudinal fasciculus. Note corticospinal tracts (*dotted arrow*) arching anteriorly toward the expected location of the motor cortex. Some fibers (*long arrow*) of the posterior limbs of the internal capsules are seen arching dorsally cranial to the frontooccipital fasciculus; these are presumed to be projection fibers to the sensory cortex on the ventrolateral portion of the holosphere.

D, On the sagittal view, some of the fibers have been removed from the frontooccipital fasciculus to allow visualization of the splenium (*arrowhead*). The dotted arrow indicates corticospinal tracts, and the long arrow indicates fused caudates.

E, On the coronal image derived from fiber tracking, the thickened dysplastic fornices are foreshortened in an anteroposterior direction. The rostral extension of the fornices divide into horizontally oriented asymmetric paramedian structures similar to the posterior projections of the anterior commissure (*arrowhead*) and a single median structure similar to the precommissural fornix (*arrow*) but thicker and longer than the usual appearance of the precommissural fornix in a neonate.

F, The fused caudates have been removed from this coronal image to allow visualization of the midline fibers connecting the frontooccipital fasciculi. The fornices can be seen dorsal to the connecting fibers. A band of transversely oriented white matter is seen over the frontal convexity (*arrow*).

rior commissure provides connection between the inferior and medial temporal lobes in the normal brain (11). Norman et al (8) have stated that the anterior commissure is absent in holoprosencephaly. Other investigators have stated that the anterior commissure, which is not related to prosencephalic cleavage (20, 22), is sometimes present in the holoprosencephalic brain. A structure presumed to represent the anterior commissure was seen by tractography in the patient reported here, though asymmetric and somewhat dysplastic.

In addition to the considerable topographic variation in the holoprosencephalic brain, there are various cortical abnormalities reported (8, 20, 22). Investigators have suggested that the cortical cytoarchitecture of the holoprosencephalic brain would dictate the course of the projection fibers that connect the cortex with the deep gray matter and brain stem (18, 20, 22). In his study of 10 holoprosencephalic brains, Yakovlev (22) noted that the gigantopyramidal cells that constitute the motor cortex were ectopically positioned within the anteromedian region of the frontal lobe over the cranial surface of the holosphere, overlaying the limbic cortex (22). The anomalous location of the motor cortex explains the ventral course of the corticospinal tracts seen with tractography. Yakovlev also commented on the presence of "granulose heterotypical cortex of the sensory type in the posterolateral and ventral portions of the holosphere" (22), which may explain the more dorsal course of some of the fibers coursing through the posterior limb of the internal capsules seen with tractography.

Fiber tracking also showed a posterior commissural structure that was very similar in appearance to the callosal splenium seen in the normal neonatal brain. Uncertainty exists in the literature about whether the callosal splenium is by definition absent in semilobar holoprosencephaly. Because a normal dorsal commissural plate can form in the absence of a rostral commissural plate, the splenium can be present in the absence of the remainder of the corpus callosum (16, 17). In the patient reported here, the posterior callosal fibers represent a preserved callosal splenium, as has been suggested by Oba and Barkovich (24).

In conclusion, diffusion tensor imaging and fiber tracking allowed in vivo depiction of anomalous gray and white matter structures in holoprosencephaly that are in agreement with reports of pathologic examination of the semilobar holoprosencephalic brain. Diffusion tensor imaging and fiber tracking provide a unique and exciting means of delineating cerebral structures heretofore requiring direct pathologic examination.

Acknowledgments

I thank Rayne Ross for manuscript preparation and Paul Mott for image acquisition and raw data processing.

References

1. Dong Q, Welsh RC, Chenevert TL, et al. **Clinical applications of diffusion tensor imaging.** *J Magn Reson Imaging* 2004;19:6–18
2. Ozarslan E, Mareci TH. **Generalized diffusion tensor imaging and analytical relations between diffusion tensor imaging and high angular resolution imaging.** *Mag Reson Med* 2003;50:955–965
3. DaSilva AFM, Tuch DS, Weigell MR, Hadjikhani N. **A primer on diffusion tensor imaging of anatomical substructures.** *Neurosurg Focus* 2003;15:1–4
4. Mori S, Crain BJ, Chacko VP, van Zijl PCM. **Three dimensional tracking of axonal projections in the brain by magnetic resonance imaging.** *Ann Neurol* 1999;45 265–269
5. Jellison BJ, Field AS, Medow J, et al. **Diffusion tensor imaging of cerebral white matter: a pictorial review of physics, fiber tract anatomy, and tumor imaging patterns.** *AJNR Am J Neuroradiol* 2004;25:356–369
6. Wakana S, Jiang H, Nagae-Poetscher LM, van Zijll PCM, Mori S. **Fiber tract-based atlas of human white matter anatomy.** *Radiology* 2004;230:77–87
7. Albayram S, Melhem ER, Mori S, Zinreich SJ, Barkovich J, Kinsman SL. **Holoprosencephaly in children: diffusion tensor MR imaging of white matter tracts of the brainstem—initial experience.** *Radiology* 2002;223:645–651
8. Norman M, McGillivray B, Kalousek D, Hill A, Poskitt K. *Congenital malformations of the brain: pathological, embryological, clinical, radiological and genetic aspects.* New York, NY: Oxford University Press; 1995;187–221
9. Mukherjee P, Miller JH, Shimony JS, et al. **Normal brain maturation during childhood: developmental trends characterized with MR.** *Radiology* 2001;221:349–358
10. Schmithorst VJ, Wilke M, Dardzinski BJ, Holland SK. **Correlation of white matter diffusivity and anisotropy during childhood and adolescence: a cross-sectional diffusion tensor imaging study.** *Radiology* 2002;222:212–221
11. Carpenter MB. *Core text of neuroanatomy,* 3rd ed. Baltimore, MD: Williams & Wilkins; 1985:323–347
12. Rakie P. **Mode of cell migration to the superficial layers of the fetal monkey cortex.** *J Comp Neurol* 1972;145:61–83
13. Rollins N, Reyes T, Chia J. **Diffusion tensor imaging in lissencephaly**. *AJNR Am J Neuroradiol* 2005;26;1583–1586
14. Roessler E, Muenke M. **Holoprosencephaly: a paradigm for the complex genetics of brain development.** *J Inher Metab Dis* 1998;21:481–497
15. Golden JA. **Towards a greater understanding of the pathogenesis of holoprosencephaly.** *Brain Dev* 1999;21:513–521
16. Takahashi T, Kinsman S, Makris N, et al. **Semilobar holoprosencephaly with midline "seam": a topologic and morphogenetic model based upon MRI analysis.** *Cereb Cortex* 2003;13:1299–1312
17. Golden JA. **Holoprosencephaly: a defect in brain patterning.** *J Neuropathol Exp Neurol* 1998;57:991–999
18. Barkovich AJ, Simon EM, Clegg NJ, Kinsman SL, Hahn JS. **Analysis of cerebral cortex in holoprosencephaly with special attention to the sylvian fissures.** *AJNR Am J Neuroradiol* 2002;23:143–150
19. Barkovich AJ. **Apparent atypical callosal dysgenesis: analysis of MR findings in six cases and their relationship to holoprosencephaly.** *AJNR Am J Neuroradiol* 1990;11:333–339
20. Probst, FP. *The prosencephalies: morphology, neuroradiological appearances and differential diagnosis.* New York, NY: Springer-Verlag; 1979:35–64
21. Simon EM, Hevner R, Pinter JD, Kinsman S, Hahn J, Barkovich AJ. **Assessment of the deep gray nuclei in holoprosencephaly.** *AJNR Am J Neuroradiol* 2000;21:1955–1961
22. Yakovlev PI. **Pathoarchitectonic studies of cerebral malformations.** *J Neuropathol Exp Neurol* 1959;18:22–55
23. Saeki N, Sunami K, Kubota M, et al. **Heavily T2-weighted MR imaging of white matter tracts in the hypothalamus: normal and pathologic demonstrations.** *AJNR Am J Neuroradiol* 2001;22:1468–1475
24. Oba H, Barkovich AJ. **Holoprosencephaly: an analysis of callosal formation and its relation to the development of the interhemispheric fissure.** *AJNR Am J Neuroradiol* 1995;16:453–460